NJC

Cite this: *New J. Chem.*, 2011, **35**, 225–234

www.rsc.org/njc

**PAPER**

# Synthesis of mesoporous metal complex-silica materials and their use as solvent-free catalysts†

**Noemi Linares,[a] Angel E. Sepúlveda,[b] María C. Pacheco,[c] Jesús R. Berenguer,*[b] Elena Lalinde,[b] Carmen Nájera[c] and Javier Garcia-Martinez*[a]**

***Received (in Gainesville, FL, USA) 1st July 2010, Accepted 19th August 2010***
**DOI: 10.1039/c0nj00509f**



Incorporation of various Pd(II) complexes into the framework of MSU-X mesoporous silica has been achieved by co-condensation using a facile solvent-free one-pot synthesis. The use of ligands with triethoxysilyl terminal groups permitted the synthesis of three different metallosilanes precursors (metal complexes with ligands containing trialkoxysilane terminal groups), which allow for the homogeneous *in situ* incorporation of metal complexes covalently bonded to the porous support. Inorganic precursor tetraethylorthosilicate was used both as silica source and as solvent for the synthesis of the complexes, avoiding the use of other organic co-solvents, making the synthesis environmentally benign. The gentle synthesis conditions used such as neutral pH, room temperature and mild ethanol extraction of the surfactant, allowed a cleaner route for the immobilization of homogeneous Pd(II) catalysts in mesoporous silica, while protecting the structural and chemical integrity of the metal complexes. For comparison purposes, monomer complexes [*trans*-$PdCl_2L_2$] (L = $NH_2(CH_2)_3Si(OEt)_3$, 4-$C_5H_4N$–$(CH_2)_2Si(OEt_3)$, $PPh_2(CH_2)_2Si(OEt)_3$) were synthesized using the same aerobic reaction conditions to those use for the co-condensation processes and fully characterized before their incorporation in the mesoporous silica. The catalytic performance of these materials was tested for the Suzuki-Miyaura reaction under solvent-free conditions. Efficient mixing of all the components was accomplished by applying either magnetic stirring or ball milling. The good yields obtained, even at room temperature, confirmed the catalytic activity of the metal complexes once incorporated into the mesoporous silica framework. The possibility to work under solvent-free conditions even with solid starting reactants, is a significant step forward in the Suzuki-Miyaura coupling reaction because its benefits in terms of cost and impact of the environment.

## Introduction

Current synthesis of metal complex-supported catalyst is based on the heterogenization of successful homogeneous catalysts.[1] The process overcomes the main limitations of homogeneous catalysts, such as recovery and recycling, and limits the loss and agglomeration of metal.[2]

Nanostructured silica materials are widely used as catalyst supports because their large surface area, controllable surface chemistry and porosity, excellent stability (chemical and thermal) and good accessibility.[3–5] Nowadays, different approaches are known to support homogeneous catalysts, from the simplest physisorption of the complexes[6,7] to the covalent attachment of their ligands in nanostructured silica supports.[8–13] Surface functionalization of mesoporous silica materials by covalent bonding of organic species on preformed silica (grafting) has become the most common approach. At present, many complexes have been heterogenized by this method, grafting one or more ligands of the complex on the support. Subsequently, these ligands are reacted with the metal to finally obtain the desired catalyst.[14–20] The main drawbacks of this approach include long time refluxing conditions in non-polar solvents and the presence of an excess of the organosilane, the poor dispersion of the complexes on the support, the difficulty to prepare and

[a] *Laboratorio de Nanotecnología Molecular, Departamento de Química Inorgánica, Universidad de Alicante, Carretera San Vicente s/n, E-03690, Alicante, Spain. E-mail: j.garcia@ua.es; Web: www.ua.es/grupo/nanolab*
[b] *Departamento de Química-Grupo de Síntesis Química de La Rioja, UA-CSIC, Universidad de La Rioja, E-26006, Logroño, Spain. Web: www.unirioja.es/dptos/dq/grupos/materiales*
[c] *Grupo de Procesos Catalíticos en Síntesis Orgánica, Departamento de Química Orgánica, Universidad de Alicante, Carretera San Vicente s/n, E-03690, Alicante, Spain*

† Electronic supplementary information (ESI) available: Fig. S1 ($N_2$ isotherms and TEM images of silica materials prepared with EtOH in the synthesis), Fig. S2 (DRUV spectra of MSU-$PdCl_2(APTS)_2$ and MSU-$PdCl_2(PPETS)_2$ materials), Fig. S3 (FT-IR spectra of MSU-$PdCl_2(APTS)_2$ and MSU-$PdCl_2(PPETS)_2$ materials), Fig. S4 (SEM and mapping images of the silica materials). CCDC reference number 777001. For ESI and crystallographic data in CIF or other electronic format see DOI: 10.1039/c0nj00509f

control certain structures, as well as the characterization of the final complex obtained.

An alternative approach to overcome these challenges involves, first, the synthesis of the desired metal complexes with terminal trialkoxysilyl groups in their ligands. Once characterized, the subsequent co-condensation of these complexes with the silica precursor during the formation of the mesoporous material yields a hybrid material in which the metal complex forms part of the silica framework in a similar way to the incorporation of organic groups in periodic mesoporous organosilica materials[21–23] (PMOs). The idea behind this method is inspired by the use of bridged organosilane precursors $(CH_3(CH_2)_nO)_3Si–R–Si(O(CH_2)_nCH_3)_3$ to smartly and homogeneously introduce different functionalities in mesostructured silicas. Recently, our group have used this approach to carry out the direct incorporation of functionalized Pd nanoparticles in a silica matrix by covalent binding, using mercaptopropyltriethoxysilane as functionalizing agent.[24]

Despite the advantages that *a priori* this method presents, such as simplicity, homogeneous distribution of the active site and better characterization of the catalytic active complex, few examples are found elsewhere.[25–31] The difficulty to preserve the complexes during the synthesis of nanostructured materials due to the synthetic conditions (high pH, hydrothermal treatment and chemical surfactant extraction) makes challenging the incorporation of metal complexes by the co-condensation method. However, since the discovery of a new strategy for the synthesis of mesoporous silica materials using neutral surfactants ($S^0N^0$) by Tanev and Pinnavaia[32] in 1994, a myriad of new mesostructures have been prepared using neutral surfactants, neutral pH and facile solvent extraction methods of the surfactants.[33–38] These milder synthesis pathways permit the incorporation of complexes by the co-condensation method.

Recently, Li and co-workers[28–30] have used this approach to synthesize different mesoporous organometalsilicas containing Au(I), Ru(II), Rh(I) or Pd(II) organometallicsilanes, which exhibited similar activity and selectivity to the related homogeneous organometallic catalysts and much higher than the corresponding immobilized catalyst obtained by grafting method. Nevertheless, organic co-solvents and thermal treatment is still required in the synthesis of these materials.

In the present work, we describe a facile aerobic, room temperature, one-pot synthesis preparation of different metalorganic/inorganic materials in which the use of a neutral surfactant for the synthesis of mesoporous MSU-X type silica has allowed the incorporation of various Pd(II) complexes containing amine, pyridine or phosphine ligands into the silica framework. Monomer complexes have been prepared under the same reaction conditions and fully characterized before the formation of the mesoporous materials by elemental analyses, spectroscopic ($^1H$, $^{13}C\{^1H\}$ and $^{31}P\{^1H\}$ NMR, FTIR, DRUV) and spectrometric techniques.

The catalytic performance of these materials has been tested in the Suzuki-Miyaura reaction under solvent-free conditions both under magnetic stirring and ball-milling conditions. The development of environmentally friendly solvent-free catalytic systems,[39–44] which, also, offer other synthetic advantages in terms of high yield, selectivity and simplicity is specially desirable. The solvent-free approximation is relatively simple if at least one of the reagents is a liquid or a gas, but when both of the substrates are solids their accessibility to the catalyst will limit the speed and yield of the reaction.[45] The use of ball-milling is widely applied for grinding minerals into fine particles and for the preparation and modification of inorganic solids.[46] In organic reactions, this technique can significantly improve the mixing of the reactants when performing reactions with solid starting materials.[47] Mild operation conditions, absence of solvents and easy work up make ball mill chemistry a really interesting option for catalytic reactions.[48] Herein, we report the use of mesoporous Pd complex-silica catalysts for the Suzuki-Miyaura reaction using solid/liquid reactants under solvent-free conditions.

## Experimental

### General considerations

IR spectra were recorded on a Nicolet Nexus FT-IR Spectrometer. For mononuclear complexes **1–3**, all the samples were prepared and recorded as Nujol mulls between polyethylene sheets and KBr pellets. All the mesoporous materials samples were prepared as pure material pellets and KBr diluted pellets. NMR spectra were recorded on a Bruker ARX 300 spectrometer; chemical shifts are reported in ppm relative to external TMS ($^1H$ and $^{13}C\{^1H\}$) or $H_3PO_4$ ($^{31}P\{^1H\}$), and coupling constants are given in Hz. Diffuse reflectance UV-vis (DRUV) data of pressed pure powder were recorded on a Shimazdu UV-3600 spectrophotometer with a Harrick praying mantis accessory, and recalculated following the Kubelka Munk function. MALDI and ES (including exact mass experiments) spectra were recorded on Microflex MALDI-TOF or micrOTOF-Q Bruker spectrometers, respectively. Elemental analyses of **1–3** were carried out with a Perkin-Elmer 2400 CHNS/O microanalyzer and the organic amounts in the catalysts were measured with elemental combustion analyses on a Carlo Erba CHNS–O EA1108 analyzer. Palladium content was determined by ICP-AES on a Perkin Elmer 7300 DV spectrometer, with the samples dissolved in aqua regia and the undissolved siliceous matter filtered off prior to analysis. Transmission electron microscopy (TEM) studies were carried out on a JEOL JEM-2010 microscope (200 kV, 0.14 nm of resolution). Samples for TEM studies were prepared by dipping a sonicated suspension of the sample in methanol on a carbon-coated copper grid. Scanning electron microscopy (SEM) images of the samples and electron energy-dispersive spectroscopy (EDS) were carried out using a Hitachi S-3000N microscope and Bruker XFlash 3001 spectrometer; for the SEM images the samples were previously covered with gold. Porous texture was characterized by $N_2$ adsorption at 77 K in an AUTOSORB-6 apparatus. The samples were previously degassed for 5 h at 373 K at $5 \times 10^{-5}$ bars. $[PdCl_2(PhCN)_2]$ was prepared as reported[49] and the rest of the reagents were used as received without further purification.

Catalytic reactions were carried out under magnetic stirring or mechanochemical ball mill conditions using a Mixer Mill

 

Retsch MM 200 model, housing two Teflon lined stainless-steel cups, each containing one Eppendorf plastic centrifuge tube with three stainless steel balls, and sealed by a stainless-steel lid fitted with a Teflon gasket. The reaction mixtures and products were analyzed by a gas chromatograph (Agilent 6890N) using a HP-5MS capillary column (fused silica, 30 m, 0.25 mm i.d.) and a flame ionization detector with decane as an internal standard.

### Synthesis of Pd(II) complexes

**Synthesis of [*trans*-$PdCl_2L_2$] (L = $NH_2(CH_2)_3Si(OEt)_3$ (APTS) 1, 4-$C_5H_4N$–$(CH_2)_2Si(OEt_3)_2$ (PETS) 2).** Orange suspensions of $[PdCl_2(PhCN)_2]$ (0.10 g, 0.26 mmol) in 5 mL of tetraethoxysilane (TEOS) were treated with 0.52 mm of the corresponding amine or pyridine ligands (122 μL of APTS or 140 μL of PETS), and the mixtures were stirred for 15 min to yield yellow solutions. Evaporation of the solutions to small volume (~1–2 mL), addition of 15 mL of hexane and cooling at −30 C for one hour caused the precipitation of complexes **1** (0.12 g, 76%) or **2** (0.14 g, 75%) as yellow solids.

**Data for 1.** Anal. found: C, 34.55; H, 7.20; N, 4.46%. $C_{18}H_{46}Cl_2N_2O_6PdSi_2$ requires C, 34.87; H, 7.48; N, 4.52%. *m*/*z* (ES+) 641.1198 (M + Na). $C_{18}H_{46}Cl_2N_2NaO_6PdSi_2$ requires 641.1204; *m*/*z* (ES+) 643 ($M^+$ + Na, 1%), 585 ($M^+$ − Cl, 7%), 385 ($M^+$ − 2Cl − $Si(OEt)_3$, 100%); $\nu_{max}$(KBr)/$cm^{-1}$ 3274s (N–H), 3231vs (N–H), 3146s, 2973vs (C–H), 2930vs (C–H), 2886vs (C–H), 1586s (N–H), 1469m (C–H), 1166vs, 1102vs, 1078vs, 814s, 793s, 770s, 483m (Pd–N), 335m (Pd–Cl); $\delta_H$(300 MHz; $CDCl_3$; $SiMe_3$) 3.82 (12H, q, $J_{H-H}$ 7.0, $^3J_{Si-H}$ 142.6, $OCH_2CH_3$), 2.79 (2H, t) and 2.76 (2H, t) ($J_{H-H}$ 6.5, $NCH_2CH_2CH_2Si$, both signals partially overlap), 2.67 (4H, m, $NH_2$), 1.73 (4H, m, $J_{H-H}$ 7.5, $NCH_2CH_2CH_2Si$), 1.23 (18H, t, $J_{H-H}$ 7.0, $^4J_{Si-H}$ 125.9, $OCH_2CH_3$), 0.63 (4H, t, $J_{H-H}$ 8, $NCH_2CH_2CH_2Si$); $\delta_C$(75.5 MHz; $CDCl_3$; $SiMe_3$) 58.4 (s, $OCH_2CH_3$); 47.5 (s, $NCH_2CH_2CH_2Si$); 24.9 (s, $NCH_2CH_2CH_2Si$); 18.3 (s, $OCH_2CH_3$); 7.3 (s, $NCH_2CH_2CH_2Si$). $\lambda_{abs,max}$(solid state diffuse reflectance)/nm 241, 341, 380.

**Data for 2.** Anal. found: C, 43.60; H, 5.85; N, 4.12%. $C_{26}H_{46}Cl_2N_2O_6PdSi_2$ requires C, 43.61; H, 6.47; N, 3.91%. *m*/*z* (ES+) 737.1198 (M + Na). $C_{26}H_{46}Cl_2N_2NaO_6PdSi_2$ requires 737.1204; *m*/*z* (MALDI+) 681 ($M^+$ − Cl, 100%); $\nu_{max}$(KBr)/$cm^{-1}$ 2974vs (C–H), 2926s (C–H), 2874s (C–H), 1615s (py), 1428vs (C–H), 1102vs, 1080vs, 817s, 785s, 669w, 443w (py); 324m (Pd–Cl), 266m (Pd–N); $\delta_H$(300 MHz; $CDCl_3$; $SiMe_3$) 8.64 (4H,d) and 7.17 (4H,d) ($J_{H-H}$ = 6.3, $C_6H_4$, py), 3.82 (12H, q, $J_{H-H}$ 7.0, $OCH_2CH_3$), 2.74 (4H, m, $CH_2CH_2Si$), 1.23 (18H, t, $J_{H-H}$ 7.0, $OCH_2CH_3$), 0.90 (4H, m, $CH_2CH_2Si$); $\delta_C$(75.5 MHz; $CDCl_3$; $SiMe_3$) 157.0 (s, $C^4$, py), 152.6 (s, $C^2$, py), 124.5 (s, $C^3$, py), 58.6 (s, $OCH_2CH_3$), 28.4 (s, $CH_2CH_2Si$), 18.3 (s, $OCH_2CH_3$), 11.0 (s, $CH_2CH_2Si$); $\lambda_{abs,max}$(solid state diffuse reflectance)/nm 238, 322, 390.

**Synthesis of [*trans*-$PdCl_2(PPETS)_2$] 3 (PPETS = $PPh_2(CH_2)_2Si(OEt)_3$).** Addition of 100 μL (0.28 mmol) of PPETS on an orange suspension of 53 mg (0.14 mmol) of $[PdCl_2(PhCN)_2]$ in 10 mL of TEOS/EtOH (1 : 1) yielded the precipitation of **3** as a yellow solid, which was filtered after 15 min of stirring (90 mg, 70%). (Found: C, 51.88; H, 5.90%. $C_{40}H_{58}Cl_2O_6P_2PdSi_2$ requires C, 51.64; H, 6.28%). *m*/*z* (ES+) 951.1551 (M + Na). $C_{40}H_{58}Cl_2NaO_6P_2PdSi_2$ requires 951.1556; *m*/*z* (MALDI+) 932 ($M^+$ − 2H, 13%), 895 ($M^+$ − Cl, 100%); $\nu_{max}$(KBr)/$cm^{-1}$ 3074m (C–H), 3060m (C–H), 2972s (C–H), 2923s (C–H), 2890s,br (C–H), 1586w (ph), 1572w (ph), 1482s (C–H), 1437vs (P–C), 1102vs, 1071vs, 769s, 736vs, 693s, 490s, 480s; 470, 348m (Pd–Cl), 247m (Pd–P); $\delta_H$(300 MHz; $CDCl_3$; $SiMe_3$) 7.70, 7.36 (20H, m, Ph), 3.73 (12H, q, $J_{H-H}$ 7.0, $OCH_2CH_3$), 2.49 (4H, m, $PCH_2CH_2Si$), 1.15 (18H, t, $J_{H-H}$ 7.0, $OCH_2CH_3$), 0.81 (4H, m, $PCH_2CH_2Si$);$\delta_C$(75.5 MHz; $CDCl_3$; $SiMe_3$) 133.8 (t, *o*-C, $^2J_{P-C}$ 5.8, $PPh_3$), 130.3 (s, *p*-C, $PPh_3$), 130.1 (pst, *i*-C, $^{1+3}J_{P-C}$ 44.9, $PPh_3$), 128.2 (t, *m*-C, $^3J_{P-C}$ 4.9, $PPh_3$), 58.5 (s, $OCH_2CH_3$), 19.1 (pst, $^{1+3}J_{P-C}$ 27.0, $PCH_2CH_2Si$), 18.2 (s, $OCH_2CH_3$), 4.3 (s, $PCH_2CH_2Si$); $\delta_P$(121.5 MHz; $CDCl_3$; $H_3PO_4$) 21.4 (s); $\lambda_{abs,max}$(solid state diffuse reflectance)/nm 210, 242, 294*sh*, 343.

### Crystal structure determination of [*trans*-$PdCl_2(PPETS)_2$] 3

Pale-yellow single crystals were obtained by slow evaporation of a toluene–hexane solution of complex **3** at room temperature. X-Ray intensity data were collected with a NONIUS κCCD area-detector diffractometer, using graphite-monochromated Mo-Kα radiation (λ 0.71073 Å). Images were

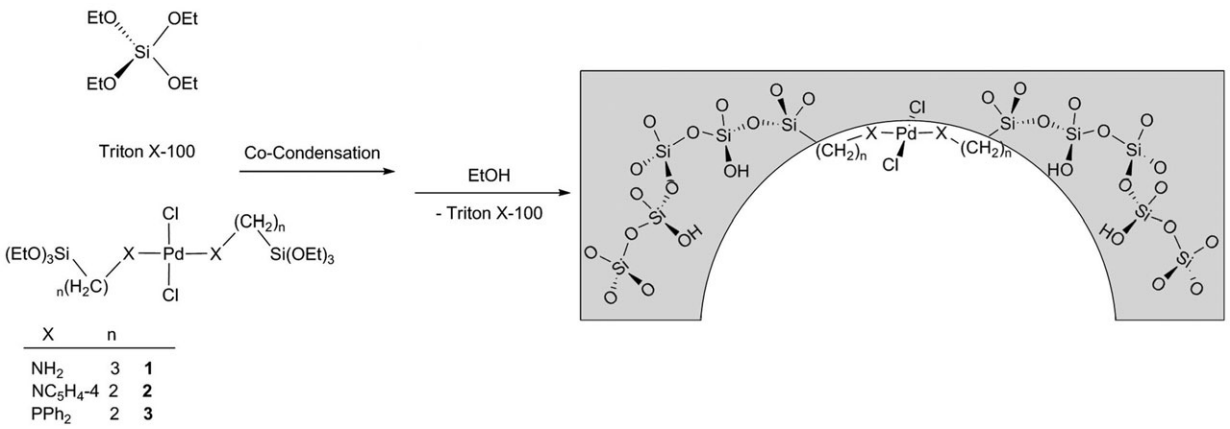


**Scheme 1** Schematic representation of the preparation of mesoporous metal complex-silica materials by surfactant directing co-condensation.

processed using the DENZO and SCALEPACK suite of programs.[50] The structures were solved by Patterson and Fourier methods using the DIRDIF92 program,[51] and the absorption correction was performed using SORTAV.[52] Rest of computation was performed with the SHELXL-97.[53] All non-hydrogen atoms were refined anisotropically.

**Crystal data.** $C_{40}H_{58}Cl_2O_6P_2PdSi_2$, $M$ = 930.28, triclinic, $a$ = 9.2480(4), $b$ = 11.4080(7), $c$ = 11.7210(8) Å, $\alpha$ = 76.248(3), $\beta$ = 71.031(4), $\gamma$ = 78.739(3)°, $V$ = 1126.49(11) Å$^3$, $T$ = 120(1) K, space group $P\bar{1}$, $Z$ = 1, 13 908 reflections measured, 4607 unique ($R_{int}$ = 0.0649). The final $R$ [$I > 2\sigma(I)$] and w$R_2$ (all data) were 0.0378 and 0.0839, respectively.

CCDC reference number 777001.

For crystallographic data in CIF or other electronic format see DOI: 10.1039/c0nj00509f

### Synthesis of mesoporous metal complex-silica catalysts

Catalysts were synthesized by co-condensation of the Pd(II) complexes **1–3** and tetraethylorthosilicate (TEOS, Aldrich) as silica sources, Triton X-100 (Alfa Aesar) was used as structure-directing agent and ammonium fluoride ($NH_4F$, Aldrich) as nucleophilic catalyst for the condensation of the silica network (Scheme 1). A reported synthesis of MSU-X type silica[54] was judiciously adapted for the incorporation of the Pd(II) complexes.

In a typical synthesis 0.58 g (0.9 mmol) of Triton X-100 was magnetically stirred in 30 g of distilled water until a clear solution was obtained. Then, 20 mg of $PdCl_2(PhCN)_2$ (0.05 mmol) was suspended in 1.9 g of TEOS (9 mmol, 1 wt% nominal Pd : $SiO_2$) and the corresponding amount of ligand was added. Orbital agitation was kept until total dissolution of the formed complex and the mixture was added dropwise to the solution of surfactant, being the two phases obtained vigorously stirred. To induce the silica precipitation 3.4 ml of a solution 0.05 M of ammonium fluoride was added. The mixture was reacted at room temperature during 24 h under vigorous stirring. The obtained solid was washed with water, ethanol and acetone in succession, filtered off, and air dried at 40 °C. Finally, the surfactant was removed by ethanol extraction (0.2 g catalyst/50 ml ethanol) at room temperature for 12 h. The samples are labelled as MSU_$PdCl_2$(APTS)$_2$, MSU_$PdCl_2$(PETS)$_2$ and MSU_$PdCl_2$(PPETS)$_2$ for the samples prepared with the Pd(II)-amine, Pd(II)-pyridine and Pd(II)-phosphine complexes, respectively.

Pd concentration in the silica materials was varied between 0.5–2.5 wt% nominal Pd : $SiO_2$, case of the pyridine complex, and 0.5–1.5 wt% nominal Pd : $SiO_2$, case of the amine and phosphine complexes. Different amounts of ethanol can be added as co-solvent to increase the solubility of complexes in the inorganic precursor until a clear solution is obtained, volume ratios between 0 : 1 and 1 : 1 (v : v) EtOH : TEOS have been tested giving similar materials (see Fig. S1 in the ESI†).

**Spectroscopic data for MSU_$PdCl_2$(APTS)$_2$.** $\nu_{max}$(KBr)/cm$^{-1}$ 3404s,br, 2955m (C–H), 2926m (C–H), 2876w (C–H), 1634s, 1513m (N–H), 1458m (C–H), 1082vs,br, 800s, 459vs; $\lambda_{abs,max}$(solid state diffuse reflectance)/nm 243, 290, 400.

**Spectroscopic data for MSU_$PdCl_2$(PETS)$_2$.** $\nu_{max}$(KBr)/cm$^{-1}$ 3437s,br, 2961m (C–H), 2926m (C–H), 2855m (C–H), 1634s, 1456w (C–H), 1082vs, 799s, 669w (py), 456vs, 278m (Pd–N); $\lambda_{abs,max}$(solid state diffuse reflectance)/nm 237, 338.

**Spectroscopic data for MSU_$PdCl_2$(PPETS)$_2$.** $\nu_{max}$(KBr)/cm$^{-1}$ 3465s,br, 2960m (C–H), 2927m (C–H), 2856w (C–H), 1639s, 1511w, 1455w (C–H), 1437w (P–C), 1085vs, 798s, 467s, 247m (Pd–P); $\lambda_{abs,max}$(solid state diffuse reflectance)/nm 208, 241, 254sh, 294, 339sh with a tail to 400.

### Catalytic test

Catalyst materials were tested in the Suzuki coupling reaction of phenylboronic acid with 1-bromonaphthalene and 4′-bromoacetophenone in the presence of $K_2CO_3$ or KOH. Reactions were carried out in air at room temperature and solvent-free conditions using magnetic stirring in the case of a liquid substrate, such as 1-bromonaphthalene. In the case of the solid 4′-bromoacetophenone the reaction was performed in a ball-milling apparatus (mechanochemical agitation). For comparison purposes, magnetic stirring and different solvents were also tested.

In a typical reaction, a mixture of phenylboronic acid (48.2 mg, 0.75 mmol), aryl bromide (0.25 mmol), base ($K_2CO_3$, 0.5 mmol) and the catalyst (see Tables 3 and 4) was stirred for the time indicated in Table 3. When ball-milling was used, the reaction mixture was introduced in an Eppendorf plastic centrifuge tube (1.5 mL) with three stainless steel balls, and sealed by a stainless-steel lid fitted with a Teflon gasket. The reaction vessel was fixed on the vibration arms of the ball-milling apparatus, along with three stainless balls of 5 mm diameter. Then, the vibration was adjusted for the reaction start, a milling cycle involving 30 min agitation periods followed by a 5 min cooling pause was selected. This milling cycle was then repeated until the reaction times showed in Table 4. Once the reaction is stopped, 10 ml of hexane was added to the mixture and the suspension was filtered off and washed with hexane and ether (10 mL). The filtrates were evaporated affording the corresponding biphenyls.

## Results and discussion

### Pd(II) complexes

Monomer complexes [*trans*-$PdCl_2L_2$] (L = $NH_2(CH_2)_3Si(OEt)_3$ APTS **1**, 4-$C_5H_4N$–$(CH_2)_2Si(OEt)_3$ PETS **2**, $PPh_2(CH_2)_2Si(OEt)_3$ PPETS **3**) were obtained by treatment of [$PdCl_2(PhCN)_2$] with the corresponding ligands in a 1 : 2 M/L ratio. In all the cases, the reactions were carried out in similar aerobic conditions to those employed for the synthesis of the catalysts (room temperature, TEOS as solvent for **1** and **2**, TEOS/EtOH 1 : 1 mixture for **3**, see Experimental), thus avoiding the use of any other organic co-solvent, not only in the synthesis of the mononuclear complexes, but also in the preparation of the hybrid mesoporous materials. Complexes **1–3** have been characterized by elemental analyses and spectroscopic ($^1$H, $^{13}$C{$^1$H} and $^{31}$P{$^1$H} NMR, FTIR, DRUV) and spectrometric means (see Experimental). Solid-state Diffuse Reflectance UV-vis spectra of complexes **1–3** display a typical intraligand broad high energy band (237–243 nm) and low

 

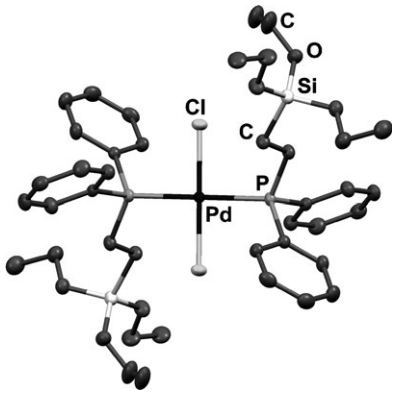


**Fig. 1** Molecular structure of [*trans*-$PdCl_2(PPETS)_2$] **3** with 50% possibility ellipsoids. Selected bond distances and angles: Pd–Cl 2.3020(7) Å, Pd–P 2.3212(7) Å, Cl–Pd–P 90.93(3)°.

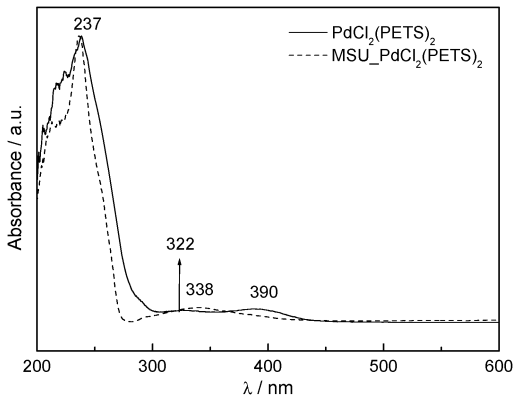


**Fig. 2** DRUV spectra of pressed pure powders of the MSU-$PdCl_2(PETS)_2$ material (dotted line) and the monomer complex [*trans*-$PdCl_2(PETS)_2$] **2** (solid line).

energy features (341, 380 nm **1**; 322, 390 nm **2**; 294, 343 nm **3**) most likely associated to metal perturbed intraligand transitions. As expected for the *trans*-configuration of the complexes, only one $\nu$(Pd–Cl) (335 **1**, 324 **2**, 348 $cm^{-1}$ **3**) and $\nu$(Pd–N) (483 **1**, 266 $cm^{-1}$ **2**) or $\nu$(Pd–P) (247 $cm^{-1}$ **3**) stretching absorption are observed in their FTIR spectra;[55] while their NMR spectra confirm the presence of only one set of signals corresponding to the amine, pyridine or phosphine ligands.

It must be noted that Li and co-workers[30] have recently reported the preparation of periodic mesoporous organometalsilicas with the incorporation of [*cis*-$PdCl_2\{PPh_2(CH_2)_2Si(OEt)_3\}]_2$, which is, in fact, an isomer of the phosphine derivative **3**. Nevertheless, the mutually *trans* disposition of the phosphine ligands in **3** has been undoubtedly confirmed, not only spectroscopically, but also with a single-crystal X-ray diffraction study, as shown in Fig. 1. We were also able to grow several pale-yellow crystals of complex [*trans*-$PdCl_2(APTS)_2$] **1**, which were subjected to single-crystal X-ray diffraction studies. The crystals were not of sufficient quality systematically, although the *trans* nature of the derivative was also unequivocally confirmed.

### Mesoporous metal complex-silica catalysts

The preparation of the hybrid mesoporous metal complex-silica catalyst is illustrated in Scheme 1. Aerobic solutions of the mononuclear derivatives **1–3** in TEOS (or TEOS : EtOH for **3**) were added to water solutions of the Triton X-100 surfactant. Ammonium fluoride was added to the mixture allowing TEOS and the silane bridged-palladium(II) complexes co-condensate for 24 h at room temperature. Finally, the surfactant was removed by treatment of the solids obtained with EtOH for 12 h at room temperature to give the mesoporous palladium complex-silica materials MSU_$PdCl_2L_2$ (L = APTS, PETS, PPETS), as observed in their FTIR spectra, which show no characteristic signals from Triton X-100.

The incorporation of the Pd(II) complexes into the mesoporous silica support can be inferred from the FTIR and DRUV spectra of the materials. Thus, the DRUV spectra of pressed pure powders of the extracted silica materials (see Fig. 2 and S2 in ESI†) show similar features to that observed for the Pd(II) complexes **1–3**, being practically identical in the case of the high-energy absorption at *ca.* 240 nm. Also, as can be seen in Fig. 3 for the pyridine material (see also Fig. S2 in ESI†), the FTIR spectra of both, complex and material, show several absorptions in the high energy region (2965–2840 $cm^{-1}$) characteristic of the $\nu$(C–H) stretching vibration of the aromatic rings and the $CH_2$ units.[29] In this zone the absorptions observed at 3274 and 3231 $cm^{-1}$ ($\nu$(N–H)) for complex **1** or at 3074 and 3060 $cm^{-1}$ ($\nu(C–H)_{Ph}$) for complex **3** are obscured by a broad band centred at *ca.* 3400 $cm^{-1}$ ($\nu$(O–H)) in the spectra of the corresponding metal complex-mesoporous silica materials. A weak absorption at *ca.* 1455 $cm^{-1}$, which could be assigned to δ(C–H) deformation vibration,[55] is also observed for the three materials. The spectra contain also other absorptions characteristic of each of the ligands employed. Thus, MSU_$PdCl_2(APTS)_2$ display one peak at 1513 $cm^{-1}$, which can be attributed to the N–H degenerate deformation $\delta_a$(H–N–H) of the $NH_2$ fragments, while MSU_$PdCl_2(PETS)_2$ shows a weak absorption at 669 $cm^{-1}$ (δ(Py)) corresponding to an in-plane ring deformation of the pyridine rings.[55] MSU-$PdCl_2(PPETS)_2$ spectrum also displays a weak signal at 1437 $cm^{-1}$ characteristic of the $\nu$(P–C) stretching vibration.[29] All this vibration modes can be also observed, appearing at very close wavenumbers, in the FTIR spectra of the monomer Pd(II) complexes (see Fig. 3 and S3 in the ESI†). By contrast, the $\nu$(Pd–Cl) observed for the three complexes (*ca.* 340 $cm^{-1}$) and the $\nu$(Pd–N) of the amino derivative **1** (483 $cm^{-1}$) are covered by the strong absorption peak of Si–O bonds (*ca.* 460 $cm^{-1}$) in the silica materials. Nevertheless, for MSU_$PdCl_2(PETS)_2$ and MSU_$PdCl_2(PPETS)_2$ one weak feature is observed in the low energy zone at 278 and 247 $cm^{-1}$, respectively, which can be ascribed to the $\nu$(Pd–N) or $\nu$(Pd–P) stretching vibrations, and correlate well with those observed for the monomer derivatives (266 $cm^{-1}$ for **2** and 247 $cm^{-1}$ for **3**).[55]

The Pd content was determined by ICP giving a 0.75 wt% loading of Pd, case of pyridine ligand, 0.70 wt% case of phosphine ligand and 0.65 wt% case of amine ligand. The presence of organic amounts in the inorganic silica network of

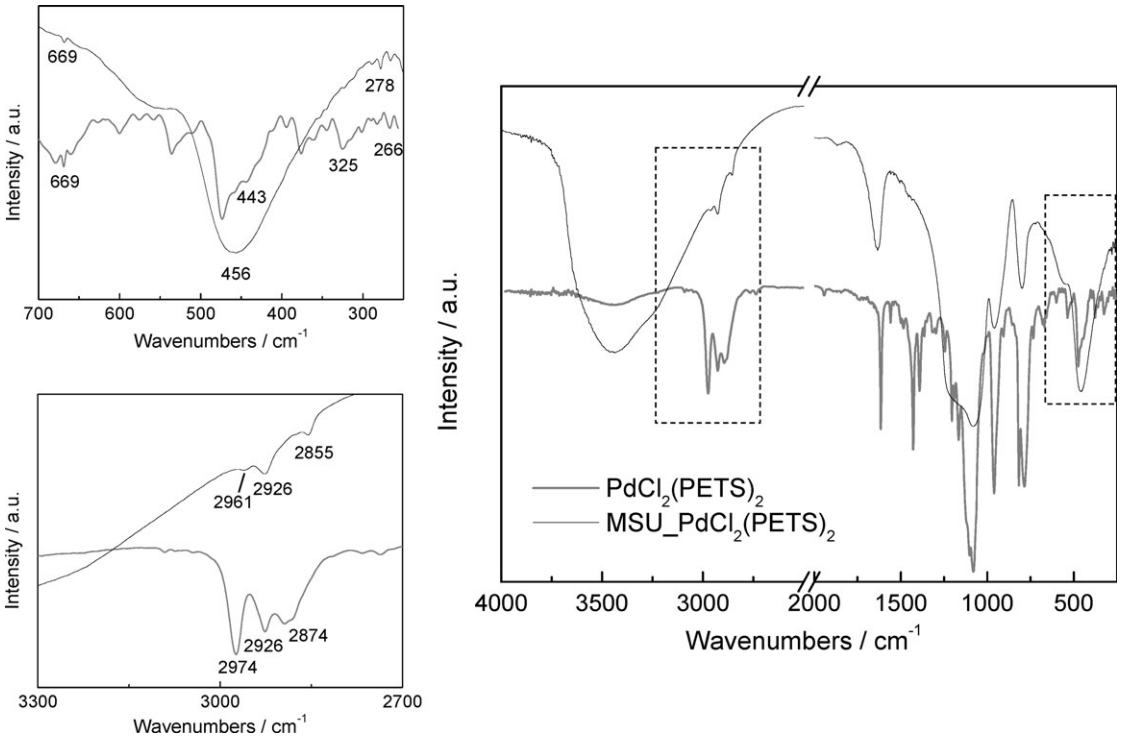


**Fig. 3** FT-IR spectra of the MSU-$PdCl_2(PETS)_2$ silica material (up) and the monomer complex [*trans*-$PdCl_2(PETS)_2$] **2** (down). For clarity, two magnifications of the marked areas in the spectrum are shown in the left.

**Table 1** Metal and organic incorporation in the mesoporous silica materials estimated by ICP-AES, elemental analysis and TGA

| Samples | Pd[a] (wt%) | N[b] (wt%) | %C[b] (wt%) | %H[b] (wt%) | N : Pd[c] (molar ratio) | %Organic content[b] (EA) | %Organic content[d] (TGA) |
|---|---|---|---|---|---|---|---|
| MSU_$PdCl_2(APTS)_2$ | 0.65 (1.0[e]) | 0.32 (0.27[e]) | 4.00 | 1.50 | 3.7 | 6% | 8% |
| MSU_$PdCl_2(PETS)_2$ | 0.75 (1.0[e]) | 0.31 (0.27[e]) | 3.40 | 1.26 | 2.8 | 5% | 8% |
| MSU_$PdCl_2(PPETS)_2$ | 0.70 (1.0[e]) | — | 3.50 | 1.30 | — | 5% | 7% |

[a] Calculated by ICP-AES analysis of the filtrate after treatment of the samples with aqua regia. [b] Determined from elemental analysis. [c] Calculated from ICP-AES and elemental analysis data. [d] Calculated from TGA after elimination of hydration water. [e] Theoretical values.

the mesoporous materials was analyzed by elemental analysis and TGA. The C, H and N content, and the calculated percentage in weight of organic species are given in Table 1. The experimental amount of N in the materials is similar to the theoretical one, suggesting the total incorporation of the ligands during the synthesis and extraction procedure. On the other hand, the N/Pd experimental molar ratios calculated from these data for samples MSU_$PdCl_2(APTS)_2$ and MSU_$PdCl_2(PETS)_2$ are over 2, which is the theoretical ratio from the starting silane bridged-Pd(II) complexes.

These differences could be attributed to the fact that the monomer complexes formation has a yield of 70–75% (see Experimental), as well as to some lost of metal during the incorporation procedure. As a result, the weakest ligand for the Pd(II), the primary amine (APTS), leads to the lowest amount of Pd loaded in the hybrid materials with identical amounts of starting Pd(II). TGA and DTA analyses (not shown here) allow to establish the amount of organic fragments incorporated in the mesoporous silica materials and their hydrothermal stability. In all cases, and after elimination of hydration water, the organic content calculated from the thermogravimetric curves for extracted materials is similar to the results obtained with the CHNS elemental analysis (see Table 1), confirming the presence of the organic ligands in the materials. DTA curves of the mesoporous metal complex-silica materials present an exothermic peak around 250–270 °C indicating the decomposing temperatures of the complexes and the similar hydrothermal stability for all of them.

Nitrogen adsorption/desorption isotherms of the mesoporous silica materials and their corresponding pore size distributions are shown in Fig. 4 and 5. For comparison purposes, the isotherm of a conventional (complex-free) MSU-X type silica is also included. All materials show type IV isotherms with a first distinctive nitrogen uptakes at $P/P_0 = 0.5$ due to the capillary condensation of nitrogen inside the mesopores. Based on the isotherms, textural parameters were calculated and listed in Table 2, being the average pore diameter around 3.5 nm in all cases, typical in these templated materials according to the size of the surfactant used in their synthesis.[56] The incorporation of the metal complexes into the MSU-X type silica materials entails the

 

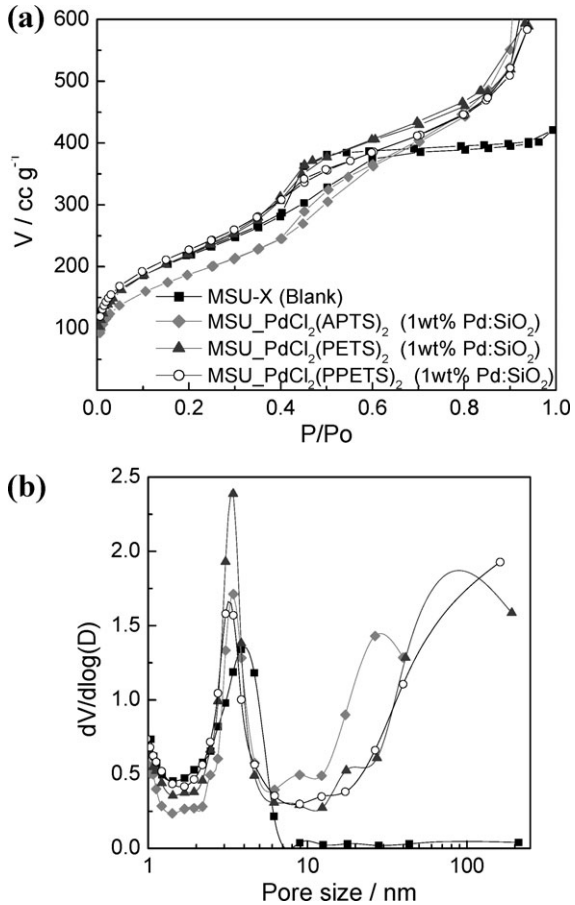


**Fig. 4** (a) $N_2$ adsorption/desorption isotherms at 77 K for catalysts $MSU\_PdCl_2(APTS)_2$ (diamonds), $MSU\_PdCl_2(PETS)_2$ (triangles) and $MSU\_PdCl_2(PPETS)_2$ (circles) with 1 wt% $Pd:SiO_2$ and for a complex-free MSU type silica (squares). (b) Their corresponding pore size distributions calculated from the adsorption branch using the BJH method.

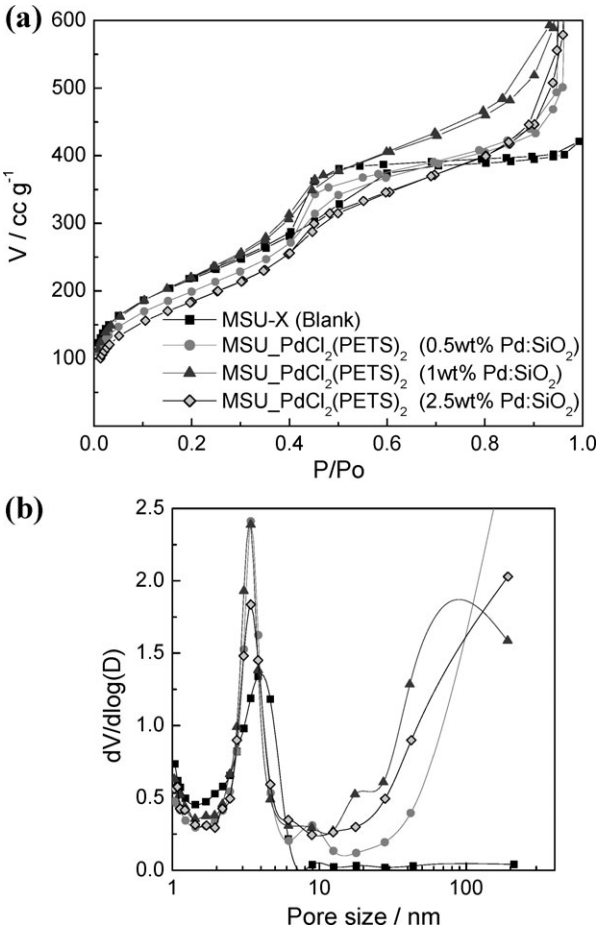


**Fig. 5** (a) $N_2$ adsorption/desorption isotherms at 77 K for catalysts $MSU\_PdCl_2(PETS)_2$ prepared with 0.5 wt% (circles), 1 wt% (triangles) and 2.5 wt% (diamonds) nominal content of $Pd:SiO_2$ and for a complex-free MSU type silica (squares). (b) Their corresponding pore size distributions calculated from the adsorption branch using the BJH method.

apparition of a second adsorption process at $P/P_0 > 0.8$, which is characteristic of textural interparticle meso/macroporosity. The bimodal porosity of the catalyst, with small (3.5 nm) mesopores and large interparticle mesopores/macropores, can be observed in both, isotherms and pore size distribution (see Fig. 4). In any case, materials prepared by co-condensation of $PdCl_2(APTS)_2$ present less sharp nitrogen-uptake steps in the small mesoporosity region with higher second adsorption steps, this trend is consistent with an increase of the initial solution pH[56] due to the ligand used for the synthesis (primary amine).

The incorporation of the metal complexes causes a slight decrease in the average pore size compared to the complex-free material; as it could be expected. Interestingly, BET surface area is not affected for the incorporation of the complexes; being in some cases even higher than in the complex-free material (see Table 2 and Fig. 5), probably due to the complementary interparticular mesoporosity.

The morphology of the mesoporous catalysts was investigated by transmission electron microscopy (TEM) and scanning electron microscopy (SEM). The catalysts exhibit non-ordered wormhole-like structures, typical of MSU-type materials (Fig. 6). The bimodal porosity of the samples was also confirmed by TEM analysis which show both small intra-particle mesopores and large interparticle meso/macropores. The combination of templated mesoporosity and interparticle meso/macroporosity in these materials is expected to increase the accessibility of bulky molecules to the interior of these very open structures, which have very interesting applications in catalysis. Moreover, TEM micrographs do not show Pd(0) nanoparticles indicating that Pd(II) is atomically dispersed and no agglomeration occurs during the synthesis and extraction procedure. TEM micrographs and DRUV spectra of mesoporous metal complex-silica materials before and after surfactant extraction confirm, respectively, the preservation of the mesostructure and chemical integrity of the metal complexes after the removal of the surfactant.

SEM micrographs of mesoporous Pd(II) complexes-silica materials (see Fig. S4 in the ESI†) show an irregular morphology formed by nanosized particles, being the materials highly homogeneous. This is consistent with the nanosized particles observed by TEM. EDS analyses and chemical mapping confirm both the presence and homogenous distribution of Pd in of all the samples.

**Table 2** Textural parameters of mesoporous metal-complex silica materials with different Pd(II) contents

| Samples | Surface area/$m^2$ $g^{-1}$[a] | Mesopore volume/$cm^3$ $g^{-1}$[b] | Interparticle volume/$cm^3$ $g^{-1}$[b] | Total pore volume/$cm^3$ $g^{-1}$[b] | Mesopore size/nm[c] | Large mesopore size/nm[c] |
|---|---|---|---|---|---|---|
| MSU (blank) | 720 | 0.65 | — | 0.65 | 3.8 | — |
| MSU_$PdCl_2$(APTS)$_2$ | 670 | 0.65 | 1.40 | 2.05 | 3.4 | 30 |
| MSU_$PdCl_2$(PETS)$_2$ | | | | | | |
| 0.5 wt% nominal Pd : $SiO_2$ | 715 | 0.50 | 1.90 | 2.40 | 3.4 | * |
| 1 wt% nominal Pd : $SiO_2$ | 750 | 0.65 | 1.75 | 2.40 | 3.4 | 80 |
| 2.5 wt% nominal Pd : $SiO_2$ | 670 | 0.50 | 2.05 | 2.55 | 3.4 | * |
| MSU_$PdCl_2$(PPETS)$_2$ | 800 | 0.65 | 1.85 | 2.50 | 3.2 | * |

* Out of range of nitrogen adsorption technique.[a] The BET surface area was estimated by using multipoint BET method using the adsorption data in the relative pressure ($P/P_0$) range of 0.05–0.30. [b] Mesopore volume was calculated from the adsorption branch of the nitrogen isotherm using the BJH method, the volume was measured at the plateau of the cumulative adsorption pore volume plot (approximately 8 nm). The total pore volume was measured at $P/P_0 = 0.99$. The pore volume of the large mesopore, interparticle volume, was estimated subtracting both values. [c] Average mesopore and large mesopore sizes were estimated from the adsorption branch of the nitrogen isotherm using the BJH method.

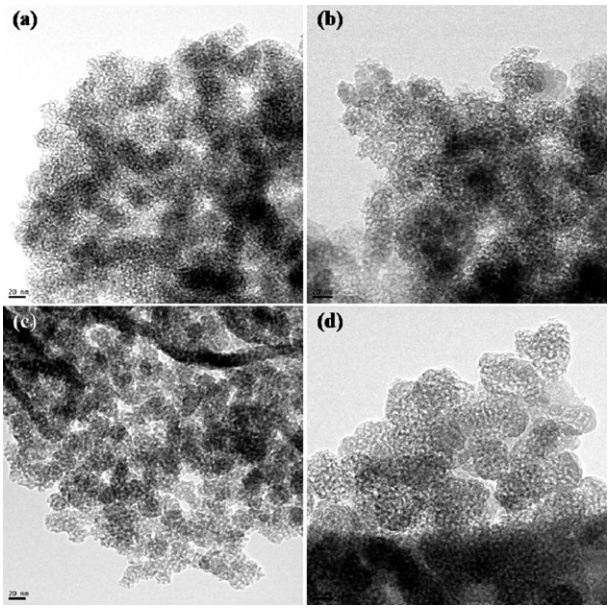


**Fig. 6** Representative TEM images of the MSU_$PdCl_2$(PETS)$_2$ material prepared from pyridine ligand and 0.75 wt% loading of Pd (a) before and (b) after surfactant extraction; (c) and (d) show the images of MSU_$PdCl_2$(APTS)$_2$ and MSU_$PdCl_2$(PPETS)$_2$ materials, respectively, prepared with 1 wt% nominal Pd : $SiO_2$ after surfactant extraction. The scale bars represent 20 nm.

### Catalytic activity

Mesoporous Pd(II) complexes-silica materials MSU_$PdCl_2$(PETS)$_2$ and MSU_$PdCl_2$(PPETS)$_2$ were tested for the Suzuki coupling reaction of phenylboronic acid with a liquid aryl bromide such as 1-bromonaphthalene (Table 3). Reactions were performed at room temperature using both different solvents and solvent-free conditions under magnetic stirring. In the case of the solid 4′-bromoacetophenone (Table 4), reactions were performed in a ball mill apparatus to improve the mixture of the solid reactants at room temperature under solvent-free conditions.

Table 3 shows the catalytic activity of the materials in the coupling reaction of phenylboronic acid with 1-bromonaphthalene using 0.1 mol% catalyst loading and $K_2CO_3$ or KOH as bases. First attempts using MSU_$PdCl_2$(PETS)$_2$ as catalyst in different solvents such as toluene, acetone and water afforded less than 2% conversion and the formation of Pd black was observed. However, under solvent-free conditions the corresponding cross-coupling took place with 41–60% of conversion after 5 h. Similar results were obtained using MSU_$PdCl_2$(PPETS)$_2$ as a catalyst. The possibility to work under solvent-free conditions significantly reduces the operating costs and the environmental impact of the process. In this case, ball-millling is less advantageous than magnetic stirring, leading to a conversion lower than 20%.

The coupling reaction of a solid reactant, namely 4′-bromoacetophenone, with phenylboronic acid requires the use of mechanochemical agitation to obtain a quantitative conversion (see Table 4). On the other hand, in the case of magnetic stirring less than 8% conversion was observed. By optimization of the reaction conditions conversion values up to 65% and 78% were obtained for Pd(II)_phosphine and Pd(II)_pyridine based silica materials, respectively. Remarkably, even with the diffusional problems associated to nanostructured silica materials in solid reactions, the use of mechanochemical agitation and Pd(II) complex-silica materials yields high levels of conversion for the coupling product of the Suzuki-Miyaura reaction.

Reproducibility in solid state reactions is always an important goal, mainly due to the heterogeneity of the mixture. At this regard, different attempts of the same reaction were carried out obtaining a better reproducibility for the material prepared with the Pd(II)-pyridine complex.

## Conclusions

Different mesoporous Pd(II) complex-silica materials were prepared, using an environmentally friendly method, by co-condensation of three metal complexes containing trialkoxysilane terminal groups with TEOS in the presence of a structure directing agent, namely Triton X-100. This synthesis strategy does not need organic co-solvents, anaerobic or anhydrous environments, being carried out at mild conditions, which preserve the integrity of the metal complexes in the silica framework. Moreover, the synthesis of the mononuclear Pd(II) complexes directly in TEOS, in the same reaction conditions than those used for the co-condensation processes, assures the correct characterization of the silane bridged-Pd(II) entities incorporated to the hybrid mesoporous material, avoiding, at the same time, the use of any additional

 

**Table 3** Catalytic activity of Pd(II) complexes-MSU materials in the coupling reaction of phenylboronic acid with 1-bromonaphthalene at RT under different conditions

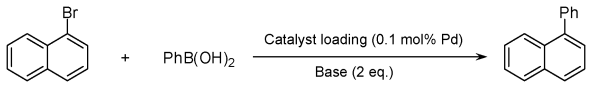


| Catalyst | $PhB(OH)_2$ (eq.) | Base | Solvent | Agitation conditions | *t*/h | Conv. (%)[a,b] |
|---|---|---|---|---|---|---|
| MSU_$PdCl_2(PETS)_2$ | 1.5 | $K_2CO_3$ | Toluene | Magnetic | 38 | 2[a] |
| | | $K_2CO_3$ | Acetone | Magnetic | 38 | 2[a] |
| | | $K_2CO_3$ | $H_2O$ | Magnetic | 38 | 1[a] |
| | | $K_2CO_3$ | No | Magnetic | 5 | 41[a] |
| | | | | | 26 | 42[a] |
| | | KOH | No | Magnetic | 5 | 60[a] |
| | | | | | 26 | 47[b] |
| MSU_$PdCl_2(PPETS)_2$ | 1.5 | $K_2CO_3$ | No | Magnetic | 5 | 56[a] |
| | | | | | 26 | 49[a] |
| | | KOH | No | Magnetic | 5 | 42[a] |
| | | | | | 26 | 47[b] |
| | 1.3 | $K_2CO_3$ | No | Mechano-chemical | 6 | 18[a] |

[a] Conversion determined by GC. [b] Isolated yield.

**Table 4** Catalytic activity of Pd(II) complexes-MSU materials in the coupling reaction of phenylboronic acid with 4′-bromoacetophenone at RT under different conditions

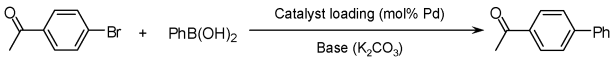


| Catalyst | Catalyst loading (mol% Pd) | $PhB(OH)_2$ (eq.) | $K_2CO_3$ (eq.) | Agitation conditions | *t*/h | Conv. (%)[a] |
|---|---|---|---|---|---|---|
| MSU_$PdCl_2(PETS)_2$ | 0.1 | 1.5 | 2 | Magnetic | 16 | 8 |
| | 0.5 | 1.5 | 2 | Mechano-chemical | 1.5 | 50 |
| | | | | | 4.5 | 75 |
| | | | | | 6 | 78 |
| | 0.5 | 2 | 3 | | 1.5 | 58 |
| MSU_$PdCl_2(PPETS)_2$ | 0.1 | 1.5 | 2 | Magnetic | 16 | — |
| | 0.25 | 2 | 3 | Mechano-chemical | 1.5 | 42 |
| | 0.25 | 1.3 | 2 | | 7 | 65 |

[a] Conversion determined by GC.

organic co-solvent (as toluene or tetrahydrofuran). The surfactant can be easily removed by ethanol extraction at room temperature without damage for the complexes, producing materials with Pd(II) complexes homogeneously and highly dispersed in a mesoporous support. The chemical integrity of the metal complexes after surfactant extraction was confirmed by spectroscopic techniques and the use of these materials as catalysts for the Suzuki-Miyaura coupling reaction of phenylboronic acid with various aryl bromides. In the case of 4′-bromoacetophenone, conversion values up to 65% and 78% were obtained for mesoporous Pd(II)_phosphine and Pd(II)_pyridine-silica materials, respectively, without the need to use any solvent. This possibility significantly reduces the costs and the environmental impact of this important reaction.

## Acknowledgements

We thank the Spanish MICINN for financial support (Projects CTQ2008-06669-C02-02 and CTQ2005-09385-C03-02) and Consolidor Ingenio 2010 CSD2007-00006. A. E. Sepúlveda thanks the UR for a grant. N.L. and M.P. are grateful for financial support under the FPI program and JdC program, respectively. A. Carrillo and E. Serrano are kindly thanked for their invaluable help during the project. Department of Applied Physics of the University of Alicante, and especially Dr Carlos Untiedt, for their continuous support.

## Notes and references

1 A. Corma and H. Garcia, *Adv. Synth. Catal.*, 2006, **348**, 1391–1412.
2 S. Brase, *et al.*, *Metal-Catalysed Cross-Coupling Reactions*, Wiley-VCH, 1998, p. 99.
3 L. Yin and J. Liebscher, *Chem. Rev.*, 2007, **107**, 133–173.
4 J. Garcia-Martinez, in *Tomorrow's Chemistry Today*, ed. B. Pignataro, Wiley-VCH, Weinheim, 2007, p. 47.
5 F. Fajula and D. Brunel, *Microporous Mesoporous Mater.*, 2001, **48**, 119–125.
6 P. C. L'Argentière, E. A. Cagnola, M. E. Quiroga and D. A. Liprandi, *Appl. Catal., A*, 2002, **226**, 253–263.
7 V. Zeleňák, V. Hornebecq and P. Llewellyn, *Microporous Mesoporous Mater.*, 2005, **83**, 125–135.
8 H. Yang, G. Zhang, X. Hong and Y. Zhu, *J. Mol. Catal. A: Chem.*, 2004, **210**, 143–148.
9 S. Jana, B. Dutta, R. Bera and S. Koner, *Langmuir*, 2007, **23**, 2492–2496.
10 R. J. P. Corriu, E. Lancelle-Beltran, A. Mehdi, C. Reye, St. Brandes and R. Guilard, *J. Mater. Chem.*, 2002, **12**, 1355–1362.
11 Y. Cao, J.-C. Hu, P. Yang, W.-L. Dai and K.-N. Fan, *Chem. Commun.*, 2003, 908–909.

12 F.-Y. Tsai, B.-N. Lin, M.-J. Chen, C.-Y. Mou and S.-T. Liu, *Tetrahedron*, 2007, **63**, 4304–4309.
13 M. P. Kapoor, W. Fujii, Y. Kasama, M. Yanagi, H. Nanbu and L. R. Juneja, *J. Mater. Chem.*, 2008, **18**, 4683–4691.
14 K. Sarkar, M. Nandi, M. Islam, M. Mubarak and A. Bhaumik, *Appl. Catal., A*, 2009, **352**, 81–86.
15 J. M. Richardson and C. W. Jones, *J. Mol. Catal. A: Chem.*, 2009, **297**, 125–134.
16 K. Komura, H. Nakamura and Y. Sugi, *J. Mol. Catal. A: Chem.*, 2008, **293**, 72–78.
17 G. Liu, M. Yao, F. Zhang, Y. Gao and H. Li, *Chem. Commun.*, 2008, 347–349.
18 C. D. Nunes, A. A. Valente, M. Pillinger, A. C. Fernandes, C. C. Romão, J. Rocha and I. S. Gonçalves, *J. Mater. Chem.*, 2002, **12**, 1735–1742.
19 W. Hao, J. Sha, S. Sheng and M. Cai, *J. Mol. Catal. A: Chem.*, 2009, **298**, 94–98.
20 J. K. Park, S.-W. Kim, T. Hyeon and B. M. Kim, *Tetrahedron: Asymmetry*, 2001, **12**, 2931–2935.
21 T. Asefa, M. J. McLacchlan, N. Coombs and G. A. Ozin, *Nature*, 1999, **402**, 867–871.
22 S. Inagaki, S. Guan, T. Ohsuna and O. Terasaki, *Nature*, 2002, **416**, 304–307.
23 S. Inagaki, S. Guan, Y. Fukushima, T. Ohsuna and O. Terasaki, *J. Am. Chem. Soc.*, 1999, **121**, 9611–9614.
24 J. Garcia-Martinez, N. Linares, S. Sinibaldi, E. Coronado and A. Ribera, *Microporous Mesoporous Mater.*, 2009, **117**, 170–177.
25 C. Baleizão, B. Gigante, D. Das, M. Alvaro, H. Garcia and A. Corma, *J. Catal.*, 2004, **223**, 106–113.
26 F. Zhang, G. Liu, W. He, H. Yin, X. Yang, H. Li, J. Zhu, H. Li and Y. Lu, *Adv. Funct. Mater.*, 2008, **18**, 3590–3597.
27 R. J. P. Corriu, A. Mehdi, C. Reyé and C. Thieuleux, *Chem. Commun.*, 2003, 1564–1565.
28 H. Li, H. Yin, F. Zhang, H. Li, Y. Huo and Y. Lu, *Environ. Sci. Technol.*, 2009, **43**, 188–194.
29 X. Yang, F. Zhu, J. Huang, F. Zhang and H. Li, *Chem. Mater.*, 2009, **21**, 4925–4933.
30 J. Huang, F. Zhu, W. He, F. Zhang, W. Wang and H. Li, *J. Am. Chem. Soc.*, 2010, **132**, 1492–1493.
31 W.-J. Zhou, B. Albela, M. Ou, P. Perriat, M.-Y. He and L. Bonneviot, *J. Mater. Chem.*, 2009, **19**, 7308–7321.
32 P. T. Tanev and T. J. Pinnavaia, *Science*, 1995, **267**, 865–867.
33 S. A. Bagshaw, E. Prouzet and T. J. Pinnavaia, *Science*, 1995, **269**, 1242–1244.
34 E. Prouzet, F. Cot, G. Nabias, A. Larbot, P. Kooyman and T. J. Pinnavaia, *Chem. Mater.*, 1999, **11**, 1498–1503.
35 R. Richer and L. Mercier, *Chem. Mater.*, 2001, **13**, 2999–3008.
36 E. Prouzet, F. Cot, C. Boissière, P. J. Kooyman and A. Larbot, *J. Mater. Chem.*, 2002, **12**, 1553–1556.
37 Y. Z. Khimyak and J. Klinowski, *J. Mater. Chem.*, 2000, **10**, 1847–1855.
38 I. Park and T. J. Pinnavaia, *Microporous Mesoporous Mater.*, 2009, **118**, 239–244.
39 Y. Chen, H. Lim, Q. Tang, Y. Gao, T. Sun, Q. Yan and Y. Yang, *Appl. Catal., A*, 2010, **380**, 55.
40 B. Karimi and D. Zareyee, *J. Mater. Chem.*, 2009, **19**, 8665.
41 C. R. Strauss, *Aust. J. Chem.*, 2009, **62**, 3.
42 P. J. Walsh, H. Li and C. Anaya de Parrodi, *Chem. Rev.*, 2007, **107**, 2503.
43 H. R. Hobbs and N. R. Thomas, *Chem. Rev.*, 2007, **107**, 2786.
44 L. Bai and J.-X. Wang, *Curr. Org. Chem.*, 2005, **9**, 535.
45 K. Tanaka and F. Toda, *Chem. Rev.*, 2000, **100**, 1025.
46 E. Colacino, P. Nun, F. Maria Colacino, J. Martinez and F. Lamaty, *Tetrahedron*, 2008, **64**, 5569.
47 S. F. Nielsen, D. Peters and O. Axelsson, *Synth. Commun.*, 2000, **30**, 3501.
48 F. Alonso, I. P. Beletskaya and M. Yus, *Tetrahedron*, 2008, **64**, 3047.
49 J. R. Doyle, P. E. Slade and H. B. Jonasseh, *Inorg. Synth.*, 1960, **6**, 218.
50 Z. Otwinowski and W. Minor, *Methods Enzymol.*, 1997, **276**, 307.
51 P. T. Beursken, G. Beursken, W. P. Bosman, de R. Gelser, S. García-Granda, R. O. Gould, J. M. M. Smith and C. Smykalla, *The DIRDIF92 program system*, Technical Report of the Crystallography Laboratory, University of Nijmegen, The Netherlands, 1992.
52 R. H. Blessing, *Acta Crystallogr., Sect. A: Found. Crystallogr.*, 1995, **51**, 33.
53 G. M. Sheldrick, *SHELX-97, a program for the refinement of crystal structures*, University of Göttingen, Germany, 1997.
54 B. Lee, H. Zhu, Z. Zhang, S. H. Overbury and S. Dai, *Microporous Mesoporous Mater.*, 2004, **70**, 71.
55 K. Nakamoto, in *Infrared and Raman Spectra of Inorganic and Coordination Compounds. Part B Applications in Coordination, Organometallic, and Bioinorganic Chemistry*, John Wiley & Sons Inc., New Jersey, 6th edn, 2009.
56 C. Boissire, A. Larbot, A. van der Lee, P. J. Kooyman and E. Prouzet, *Chem. Mater.*, 2000, **12**, 2902–2913.


 